



Precision measurement of CP violation in $B_s^0 \rightarrow J/\psi K^+ K^-$ decays

The LHCb collaboration[†]

Abstract

The time-dependent CP asymmetry in $B_s^0 \rightarrow J/\psi K^+ K^-$ decays is measured using pp collision data, corresponding to an integrated luminosity of 3.0 fb^{-1} , collected with the LHCb detector at centre-of-mass energies of 7 and 8 TeV. In a sample of 96 000 $B_s^0 \rightarrow J/\psi K^+ K^-$ decays, the CP -violating phase ϕ_s is measured, as well as the decay widths Γ_L and Γ_H of the light and heavy mass eigenstates of the B_s^0 - \bar{B}_s^0 system. The values obtained are $\phi_s = -0.058 \pm 0.049 \pm 0.006$ rad, $\Gamma_s \equiv (\Gamma_L + \Gamma_H)/2 = 0.6603 \pm 0.0027 \pm 0.0015 \text{ ps}^{-1}$, and $\Delta\Gamma_s \equiv \Gamma_L - \Gamma_H = 0.0805 \pm 0.0091 \pm 0.0032 \text{ ps}^{-1}$, where the first uncertainty is statistical and the second systematic. These are the most precise single measurements of those quantities to date. A combined analysis with $B_s^0 \rightarrow J/\psi \pi^+ \pi^-$ decays gives $\phi_s = -0.010 \pm 0.039$ rad. All measurements are in agreement with the Standard Model predictions. For the first time the phase ϕ_s is measured independently for each polarisation state of the $K^+ K^-$ system and shows no evidence for polarisation dependence.

Submitted to Phys. Rev. Lett.

[†]Authors are listed at the end of this Letter.

The CP -violating phase ϕ_s arises in the interference between the amplitudes of B_s^0 mesons decaying via $b \rightarrow c\bar{c}s$ transitions to CP eigenstates directly and those decaying after oscillation. In the Standard Model (SM), ignoring sub-leading contributions, this phase is predicted to be $-2\beta_s$, where $\beta_s = \arg[-(V_{ts}V_{tb}^*)/(V_{cs}V_{cb}^*)]$ and V_{ij} are elements of the quark-mixing matrix [1]. Global fits to experimental data give $-2\beta_s = -0.0363 \pm 0.0013$ rad [2]. This phase could be modified if non-SM particles were to contribute to the B_s^0 - \bar{B}_s^0 oscillations [3, 4] and a measurement of ϕ_s significantly different from the SM prediction would provide unambiguous evidence for processes beyond the SM.

The LHCb collaboration has previously reported measurements of ϕ_s using $B_s^0 \rightarrow J/\psi K^+ K^-$ and $B_s^0 \rightarrow J/\psi \pi^+ \pi^-$ decays [5, 6]. These measurements were based upon data, corresponding to an integrated luminosity of up to 1.0 fb^{-1} , collected in pp collisions at a centre-of-mass energy of 7 TeV in 2011 at the LHC. The ATLAS, CDF and D0 collaborations have also measured ϕ_s in $B_s^0 \rightarrow J/\psi K^+ K^-$ decays [7–9]. This Letter extends the LHCb measurements in the $B_s^0 \rightarrow J/\psi K^+ K^-$ channel by adding data corresponding to 2.0 fb^{-1} of integrated luminosity collected at 8 TeV in 2012, and presents the combined results for ϕ_s including the analysis of $B_s^0 \rightarrow J/\psi \pi^+ \pi^-$ decays from Ref. [10]. For the first time, the CP -violating phases are measured separately for each polarisation state of the $K^+ K^-$ system. Knowledge of these parameters is an important step towards the control of loop-induced effects to the decay amplitude, which could potentially be confused with non-SM contributions to B_s^0 - \bar{B}_s^0 mixing [11]. The analysis of the $B_s^0 \rightarrow J/\psi K^+ K^-$ channel reported here is as described in Ref. [6], to which the reader is referred for details, except for the changes described below.

The LHCb detector is a single-arm forward spectrometer covering the pseudorapidity range $2 < \eta < 5$, designed for the study of particles containing b or c quarks, and is described in Ref. [12]. The trigger [13] consists of a hardware stage, based on information from the calorimeter and muon systems, followed by a software stage, in which all charged particles with transverse momentum greater than 500 (300) MeV/ c are reconstructed for 2011 (2012) data. Further selection requirements are applied offline, as described in Ref. [6], in order to increase the signal purity.

The $B_s^0 \rightarrow J/\psi K^+ K^-$ decay proceeds predominantly via $B_s^0 \rightarrow J/\psi \phi$, in which the $K^+ K^-$ pair from the ϕ is in a P-wave configuration. The final state is a superposition of CP -even and CP -odd states depending upon the relative orbital angular momentum of the J/ψ and ϕ mesons. The $J/\psi K^+ K^-$ final state can also be produced with $K^+ K^-$ pairs in a CP -odd S-wave configuration [14]. The measurement of ϕ_s requires the CP -even and CP -odd components to be disentangled by analysing the distribution of the reconstructed decay angles of the final-state particles. In this analysis the decay angles are defined in the helicity basis, $\cos \theta_K$, $\cos \theta_\mu$, and φ_h , as described in Ref. [6].

The invariant mass distributions for $K^+ K^-$ and $J/\psi (\rightarrow \mu^+ \mu^-) K^+ K^-$ candidates are shown in Figs. 1(a) and 1(b), respectively. The combinatorial background is modelled with an exponential function and the B_s^0 signal shape is parameterised by a double-sided Hypatia function [15]. The fitted signal yield is $95\,690 \pm 350$. In addition to the combinatorial background, studies of the data in sidebands of the $m(J/\psi K^+ K^-)$ spectrum

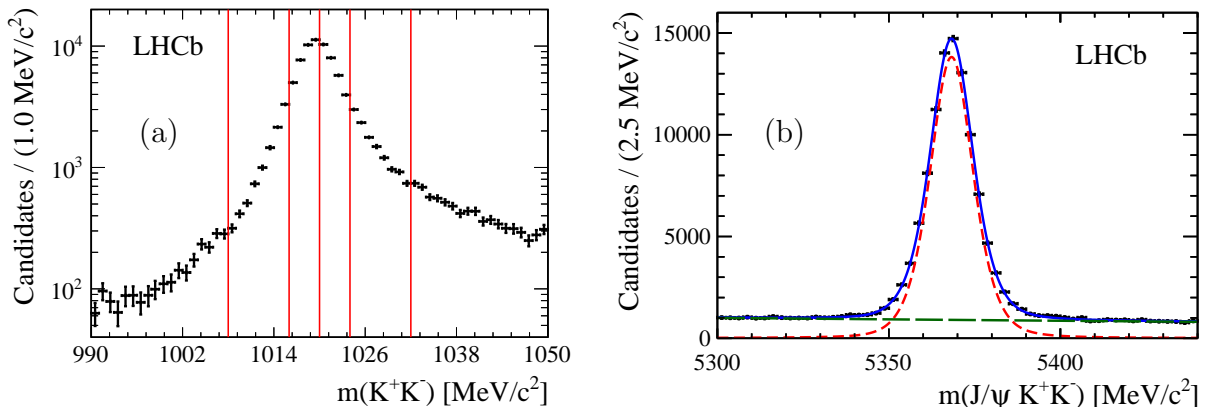


Figure 1: (a) Background-subtracted invariant mass distributions of the K^+K^- system in the selected $B_s^0 \rightarrow J/\psi K^+K^-$ candidates (black points). The vertical red lines denote the boundaries of the six bins used in the maximum likelihood fit. (b) Distribution of $m(J/\psi K^+K^-)$ for the data sample (black points) and projection of the maximum likelihood fit (blue line). The B_s^0 signal component is shown by the red dashed line and the combinatorial background by the green long-dashed line. Background from misidentified B^0 and Λ_b^0 decays is subtracted, as described in the text.

show contributions from approximately 1700 $B^0 \rightarrow J/\psi K^+\pi^-$ (4800 $\Lambda_b^0 \rightarrow J/\psi pK^-$) decays where the pion (proton) is misidentified as a kaon. These background events have complicated correlations between the angular variables and $m(J/\psi K^+K^-)$. In order to avoid the need to describe explicitly such correlations in the analysis, the contributions from these backgrounds are statistically subtracted by adding to the data simulated events of these decays with negative weight. Prior to injection, the simulated events are weighted such that the distributions of the relevant variables used in the fit, and their correlations, match those of data.

The principal physics parameters of interest are Γ_s , $\Delta\Gamma_s$, ϕ_s , $|\lambda|$, the B_s^0 mass difference, Δm_s , and the polarisation amplitudes $A_k = |A_k|e^{-i\delta_k}$, where the indices $k \in \{0, \parallel, \perp, S\}$ refer to the different polarisation states of the K^+K^- system. The sum $|A_{\parallel}|^2 + |A_0|^2 + |A_{\perp}|^2$ equals unity and by convention δ_0 is zero. The parameter λ describes CP violation in the interference between mixing and decay and is defined by $\eta_k(q/p)(\bar{A}_k/A_k)$, where it is assumed to be the same for all polarisation states. The complex parameters $p = \langle B_s^0 | B_L \rangle$ and $q = \langle \bar{B}_s^0 | B_L \rangle$ describe the relation between mass and flavour eigenstates and η_k is the CP eigenvalue of the polarisation state k . The CP -violating phase is defined by $\phi_s \equiv -\arg \lambda$. In the absence of CP violation in decay, $|\lambda| = 1$. CP violation in B_s^0 -meson mixing is negligible, following measurements in Ref. [16]. Measurements of the above parameters are obtained from a weighted maximum likelihood fit [17] to the decay-time and helicity angle distributions of the data as described in Ref. [6].

The B_s^0 decay-time distribution is distorted by the trigger selection requirements and

by the track reconstruction algorithms. Corrections are determined from data using the methods described in Ref. [18] and are incorporated in the maximum likelihood fit by a parameterised function, in the case of the trigger, and by per-candidate weights, in the case of the track reconstruction. Both corrections are validated using a sample of 10^6 simulated $B_s^0 \rightarrow J/\psi \phi$ events.

To account for the experimental decay-time resolution, the signal probability density function (PDF) is defined per candidate and is convolved with the sum of two Gaussian functions with a common mean, μ , and independent widths w_i , $i \in \{1, 2\}$. The widths are given by $w_i \equiv r_i \sigma + s_i \sigma^2$, where r_i and s_i are scale factors for each Gaussian function and σ is the per candidate decay-time uncertainty, estimated by the kinematic fit used to calculate the decay time. The scale factors are determined from the decay-time distribution of a control sample of $J/\psi K^+ K^-$ candidates that are selected as for signal except for decay-time requirements. The average value of the σ distribution in the sample of prompt candidates is approximately 35 fs and the effective average resolution is 46 fs.

The flavour of the B_s^0 candidate at production is inferred using two independent classes of flavour tagging algorithms, the opposite-side (OS) tagger and the same-side kaon (SSK) tagger, which exploit specific features of the production of $b\bar{b}$ quark pairs in pp collisions. The OS tagger algorithm is described in Ref. [6] but is re-calibrated using data sets of flavour-specific decays, yielding a tagging power of $(1.19 \pm 0.06)\%$ for events with only an OS-tag. The SSK algorithm deduces the signal production flavour by exploiting charge-flavour correlations of the kaons produced during the hadronisation process of the \bar{b} quark forming the signal B_s^0 meson. The tagging kaon is identified using a selection based on a neural network that gives an effective tagging power of $(0.84 \pm 0.11)\%$, corresponding approximately to a 40% improvement in tagging power with respect to that in Refs. [6, 19]. The SSK algorithm is calibrated using a sample of $B_s^0 \rightarrow D_s^- \pi^+$ decays. For events that have both OS and SSK tagging decisions, corresponding to 26% of the tagged sample, the effective tagging power is $(1.70 \pm 0.08)\%$. The combined tagging power of the three independent tagging categories defined above is $(3.73 \pm 0.15)\%$.

Due to different $m(K^+ K^-)$ line shapes of the S- and P-wave contributions, their interferences are suppressed by an effective coupling factor after integrating over a finite $m(K^+ K^-)$ region. The fit is carried out in six bins of $m(K^+ K^-)$, as shown in Fig. 1(a), to allow measurement of the small S-wave amplitude in each bin and to minimise correction factors in the interference terms of the PDF.

The results of the fit are consistent with the measurements reported in Ref. [6] and are reported in Table 1 where the first uncertainty is statistical and the second systematic. The correlation matrix is given in Ref. [20]. In contrast to Ref. [6] the value of Δm_s is unconstrained in this fit, thereby providing an independent measurement of this quantity, which is consistent with the results of Ref. [21]. The projections of the decay time and angular distributions are shown in Fig. 2.

The results reported in Table 1 are obtained with the assumption that ϕ_s and $|\lambda|$ are independent of the final-state polarisation. This condition can be relaxed to allow the measurement of ϕ_s^k and $|\lambda^k|$ separately for each polarisation, following the formalism in Ref. [22]. The results of this fit are shown in Table 2 and the statistical correlation matrix

Table 1: Values of the principal physics parameters determined from the polarisation-independent fit.

Parameter	Value
Γ_s [ps ⁻¹]	$0.6603 \pm 0.0027 \pm 0.0015$
$\Delta\Gamma_s$ [ps ⁻¹]	$0.0805 \pm 0.0091 \pm 0.0032$
$ A_\perp ^2$	$0.2504 \pm 0.0049 \pm 0.0036$
$ A_0 ^2$	$0.5241 \pm 0.0034 \pm 0.0067$
δ_\parallel [rad]	$3.26^{+0.10}_{-0.17} {}^{+0.06}_{-0.07}$
δ_\perp [rad]	$3.08^{+0.14}_{-0.15} \pm 0.06$
ϕ_s [rad]	$-0.058 \pm 0.049 \pm 0.006$
$ \lambda $	$0.964 \pm 0.019 \pm 0.007$
Δm_s [ps ⁻¹]	$17.711^{+0.055}_{-0.057} \pm 0.011$

Table 2: Values of the polarisation-dependent parameters ϕ_s^k and $|\lambda^k|$ determined from the polarisation-dependent fit.

Parameter	Value
$ \lambda^0 $	$1.012 \pm 0.058 \pm 0.013$
$ \lambda^\parallel/\lambda^0 $	$1.02 \pm 0.12 \pm 0.05$
$ \lambda^\perp/\lambda^0 $	$0.97 \pm 0.16 \pm 0.01$
$ \lambda^S/\lambda^0 $	$0.86 \pm 0.12 \pm 0.04$
ϕ_s^0 [rad]	$-0.045 \pm 0.053 \pm 0.007$
$\phi_s^\parallel - \phi_s^0$ [rad]	$-0.018 \pm 0.043 \pm 0.009$
$\phi_s^\perp - \phi_s^0$ [rad]	$-0.014 \pm 0.035 \pm 0.006$
$\phi_s^S - \phi_s^0$ [rad]	$0.015 \pm 0.061 \pm 0.021$

is given in Ref. [20]. There is no evidence for a polarisation-dependent CP violation arising in $B_s^0 \rightarrow J/\psi K^+ K^-$ decays.

A summary of systematic uncertainties is reported in Tables 3 and 4. The tagging parameters are constrained in the fit and therefore their associated systematic uncertainties contribute to the statistical uncertainty of each parameter in Table 1. This contribution is 0.004 rad to the statistical uncertainty on ϕ_s ; 0.004 ps⁻¹ to that of Δm_s ; 0.01 rad to that of δ_\parallel and is negligible for all other parameters.

The assumption that the $m(J/\psi K^+ K^-)$ distribution is independent from the decay time and angles is tested by re-evaluating the signal weights in bins of the decay time and angles and repeating the fit. The difference in fit results is assigned as a systematic uncertainty. The systematic effect from the statistical uncertainty on the signal weights is determined by re-computing them after varying the parameters of the $m(J/\psi K^+ K^-)$ fit model within their statistical uncertainties, and assigning the difference in fit results as a systematic uncertainty.

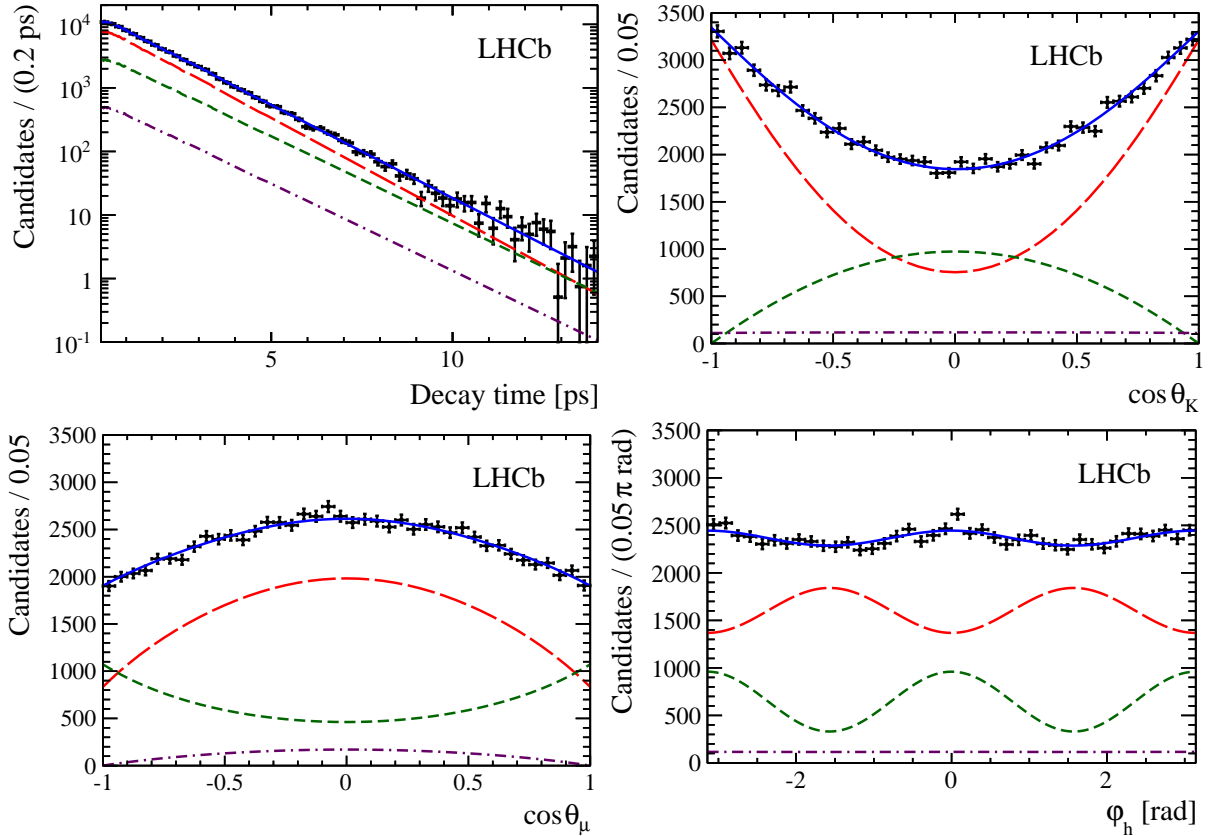


Figure 2: Decay-time and helicity-angle distributions for $B_s^0 \rightarrow J/\psi K^+ K^-$ decays (data points) with the one-dimensional fit projections overlaid. The solid blue line shows the total signal contribution, which is composed of CP -even (long-dashed red), CP -odd (short-dashed green) and S-wave (dotted-dashed purple) contributions.

The effect due to the b -hadron background contributions is evaluated by varying the proportion of simulated background events included in the fit by one standard deviation of their measured fractions. In addition, a further systematic uncertainty is assigned as the difference between the results of the fit to weighted or non-weighted data.

A small fraction of $B_s^0 \rightarrow J/\psi K^+ K^-$ decays come from the decays of B_c^+ mesons [23]. The effect of ignoring this component in the fit is evaluated using simulated pseudoexperiments where a 0.8% contribution [23, 24] of B_s^0 -from- B_c^+ decays is added from a simulated sample of $B_c^+ \rightarrow B_s^0(\rightarrow J/\psi \phi)\pi^+$ decays. Neglecting the B_c^+ component leads to a bias on Γ_s of 0.0005 ps^{-1} , which is added as a systematic uncertainty. Other parameters are unaffected.

The decay angle resolution is found to be of the order of 20 mrad in simulated events. The result of pseudoexperiments shows that ignoring this effect in the fit only leads to small biases in the polarisation amplitudes, which are assigned as systematic uncertainties.

The angular efficiency correction is determined from simulated signal events weighted as in Ref. [6] such that the kinematic distributions of the final state particles match those

Table 3: Statistical and systematic uncertainties for the polarisation-independent result.

Source	Γ_s [ps ⁻¹]	$\Delta\Gamma_s$ [ps ⁻¹]	$ A_\perp ^2$	$ A_0 ^2$	δ_\parallel [rad]	δ_\perp [rad]	ϕ_s [rad]	$ \lambda $	Δm_s [ps ⁻¹]
Total stat. uncertainty	0.0027	0.0091	0.0049	0.0034	$^{+0.10}_{-0.17}$	$^{+0.14}_{-0.15}$	0.049	0.019	$^{+0.055}_{-0.057}$
Mass factorisation	–	0.0007	0.0031	0.0064	0.05	0.05	0.002	0.001	0.004
Signal weights (stat.)	0.0001	0.0001	–	0.0001	–	–	–	–	–
b -hadron background	0.0001	0.0004	0.0004	0.0002	0.02	0.02	0.002	0.003	0.001
B_c^+ feed-down	0.0005	–	–	–	–	–	–	–	–
Angular resolution bias	–	–	0.0006	0.0001	$^{+0.02}_{-0.03}$	0.01	–	–	–
Ang. efficiency (reweighting)	0.0001	–	0.0011	0.0020	0.01	–	0.001	0.005	0.002
Ang. efficiency (stat.)	0.0001	0.0002	0.0011	0.0004	0.02	0.01	0.004	0.002	0.001
Decay-time resolution	–	–	–	–	–	0.01	0.002	0.001	0.005
Trigger efficiency (stat.)	0.0011	0.0009	–	–	–	–	–	–	–
Track reconstruction (simul.)	0.0007	0.0029	0.0005	0.0006	$^{+0.01}_{-0.02}$	0.002	0.001	0.001	0.006
Track reconstruction (stat.)	0.0005	0.0002	–	–	–	–	–	–	0.001
Length and momentum scales	0.0002	–	–	–	–	–	–	–	0.005
S-P coupling factors	–	–	–	–	0.01	0.01	–	0.001	0.002
Fit bias	–	–	0.0005	–	–	0.01	–	0.001	–
Quadratic sum of syst.	0.0015	0.0032	0.0036	0.0067	$^{+0.06}_{-0.07}$	0.06	0.006	0.007	0.011

Table 4: Statistical and systematic uncertainties for the polarisation-dependent result.

Source	$ \lambda^0 $	$ \lambda^\parallel/\lambda^0 $	$ \lambda^\perp/\lambda^0 $	$ \lambda^S/\lambda^0 $	ϕ_s^0 [rad]	$\phi_s^\parallel - \phi_s^0$ [rad]	$\phi_s^\perp - \phi_s^0$ [rad]	$\phi_s^S - \phi_s^0$ [rad]
Total stat. uncertainty	0.058	0.12	0.16	0.12	0.053	0.043	0.035	0.061
Mass factorisation	0.010	0.04	0.01	0.03	0.003	0.005	0.003	0.016
b -hadron background	0.002	0.01	–	0.01	0.003	0.001	0.001	0.009
Ang. efficiency (reweighting)	–	–	–	0.02	0.001	0.002	0.001	0.007
Ang. efficiency (stat.)	0.004	0.02	0.01	0.01	0.004	0.007	0.005	0.004
Decay-time resolution	0.006	0.01	–	0.01	0.003	0.002	0.001	0.002
S-P coupling factors	–	–	–	–	–	–	–	0.006
Quadratic sum of syst.	0.013	0.05	0.01	0.04	0.007	0.009	0.006	0.021

in the data. A systematic uncertainty is assigned as the difference between the fit results using angular corrections from weighted or non-weighted simulated events. The limited size of the simulated sample leads to an additional systematic uncertainty.

The systematic uncertainty from the decay time resolution parameters is not included in the statistical uncertainty of each parameter and is now quoted explicitly. It is assigned as the difference of fit parameters obtained from the nominal fit and a fit where the resolution model parameters are calibrated using a sample of simulated prompt- J/ψ events.

The trigger decay-time efficiency model, described in Ref. [6], introduces a systematic

uncertainty that is determined by fixing the value of each model parameter in the fit and subsequently repeating the fit with the parameter values constrained within their statistical uncertainty. The quadratic differences of the uncertainties returned by each fit are then assigned as systematic uncertainties. The systematic effect of the track reconstruction efficiency is evaluated by applying the same techniques on a large simulated sample of $B_s^0 \rightarrow J/\psi \phi$ decays. The differences between the generation and fitted values of each physics parameter in this sample is assigned as the systematic uncertainty. The limited size of the control sample used to determine the track reconstruction efficiency parameterisation leads to an additional systematic uncertainty.

The uncertainty on the longitudinal coordinate of the LHCb vertex detector is found from survey data and leads to an uncertainty on Γ_s and $\Delta\Gamma_s$ of 0.020%, with other parameters being unaffected. The momentum scale uncertainty is at most 0.022% [21], which only affects Δm_s .

Different models of the S-wave line-shape and $m(K^+K^-)$ resolution are used to evaluate the coupling factors in each of the six $m(K^+K^-)$ bins and the resulting variation of the fit parameters are assigned as systematic uncertainties. Possible biases of the fitting procedure are studied by generating and fitting many simulated pseudoexperiments of equivalent size to the data. The resulting biases are small, and those that are significantly different from zero are assigned as systematic uncertainties.

The systematic correlations between parameters are evaluated by assuming that parameters are fully (anti)correlated when the systematic uncertainty is determined by comparing results obtained from the nominal and a modified fit. Other sources of systematic uncertainty are assumed to have negligible parameter correlations. The combined statistical and systematic correlation matrix is given in Ref. [20].

A measurement of ϕ_s and $|\lambda|$ by LHCb using $B_s^0 \rightarrow J/\psi \pi^+ \pi^-$ decays of $\phi_s^{\pi\pi} = 0.070 \pm 0.068 \pm 0.008$ rad and $|\lambda^{\pi\pi}| = 0.89 \pm 0.05 \pm 0.01$, consistent with the measurement reported here, was reported in Ref. [10]. The results from the two analyses are combined by incorporating the $B_s^0 \rightarrow J/\psi K^+ K^-$ result as a correlated Gaussian constraint in the $B_s^0 \rightarrow J/\psi \pi^+ \pi^-$ fit, under the assumption that $B_s^0 \rightarrow J/\psi \pi^+ \pi^-$ and $B_s^0 \rightarrow J/\psi K^+ K^-$ decays both proceed dominantly via $b \rightarrow c\bar{c}s$ transitions and the ratio between loop-induced processes and tree diagrams are the same in each mode. The fit accounts for correlations between common parameters and correlations between systematic uncertainties. The combined result is $\phi_s = -0.010 \pm 0.039$ rad and $|\lambda| = 0.957 \pm 0.017$. The correlation between the parameters is about -0.02 .

In conclusion, the CP -violating phase ϕ_s , and the B_s^0 decay width parameters Γ_s and $\Delta\Gamma_s$, are measured using $B_s^0 \rightarrow J/\psi K^+ K^-$ decays selected from the full LHCb data set from the first LHC operation period. The results are $\phi_s = -0.058 \pm 0.049 \pm 0.006$ rad, $|\lambda| = 0.964 \pm 0.019 \pm 0.007$, $\Gamma_s = 0.6603 \pm 0.0027 \pm 0.0015$ ps $^{-1}$ and $\Delta\Gamma_s = 0.0805 \pm 0.0091 \pm 0.0032$ ps $^{-1}$. The parameter $|\lambda|$ is consistent with unity, implying no evidence for CP violation in $B_s^0 \rightarrow J/\psi K^+ K^-$ decays. For the first time, the polarisation-dependent CP -violating parameters are measured and show no significant difference between the four polarisation states. The measurements of ϕ_s and $|\lambda|$ in $B_s^0 \rightarrow J/\psi K^+ K^-$ decays are consistent with those measured in $B_s^0 \rightarrow J/\psi \pi^+ \pi^-$ decays, and the combined results are

$\phi_s = -0.010 \pm 0.039$ rad and $|\lambda| = 0.957 \pm 0.017$. The measurement of the CP violating phase ϕ_s is the most precise to date and is in agreement with the SM prediction [2], in which it is assumed that sub-leading contributions to the decay amplitude are negligible.

We express our gratitude to our colleagues in the CERN accelerator departments for the excellent performance of the LHC. We thank the technical and administrative staff at the LHCb institutes. We acknowledge support from CERN and from the national agencies: CAPES, CNPq, FAPERJ and FINEP (Brazil); NSFC (China); CNRS/IN2P3 (France); BMBF, DFG, HGF and MPG (Germany); SFI (Ireland); INFN (Italy); FOM and NWO (The Netherlands); MNiSW and NCN (Poland); MEN/IFA (Romania); MinES and FANO (Russia); MinECo (Spain); SNSF and SER (Switzerland); NASU (Ukraine); STFC (United Kingdom); NSF (USA). The Tier1 computing centres are supported by IN2P3 (France), KIT and BMBF (Germany), INFN (Italy), NWO and SURF (The Netherlands), PIC (Spain), GridPP (United Kingdom). We are indebted to the communities behind the multiple open source software packages on which we depend. We are also thankful for the computing resources and the access to software R&D tools provided by Yandex LLC (Russia). Individual groups or members have received support from EPLANET, Marie Skłodowska-Curie Actions and ERC (European Union), Conseil général de Haute-Savoie, Labex ENIGMASS and OCEVU, Région Auvergne (France), RFBR (Russia), XuntaGal and GENCAT (Spain), Royal Society and Royal Commission for the Exhibition of 1851 (United Kingdom).

References

- [1] M. Kobayashi and T. Maskawa, *CP violation in the renormalizable theory of weak interaction*, Prog. Theor. Phys. **49** (1973) 652; N. Cabibbo, *Unitary symmetry and leptonic decays*, Phys. Rev. Lett. **10** (1963) 531.
- [2] J. Charles *et al.*, *Predictions of selected flavour observables within the Standard Model*, Phys. Rev. **D84** (2011) 033005, [arXiv:1106.4041](https://arxiv.org/abs/1106.4041), with updated results and plots available at <http://ckmfitter.in2p3.fr>.
- [3] A. J. Buras, *Flavour theory: 2009*, PoS **EPS-HEP2009** (2009) 024, [arXiv:0910.1032](https://arxiv.org/abs/0910.1032).
- [4] C.-W. Chiang *et al.*, *New physics in $B_s^0 \rightarrow J/\psi\phi$: A general analysis*, JHEP **04** (2010) 031, [arXiv:0910.2929](https://arxiv.org/abs/0910.2929).
- [5] LHCb collaboration, R. Aaij *et al.*, *Measurement of the CP-violating phase ϕ_s in the decay $B_s^0 \rightarrow J/\psi\phi$* , Phys. Rev. Lett. **108** (2012) 101803, [arXiv:1112.3183](https://arxiv.org/abs/1112.3183).
- [6] LHCb collaboration, R. Aaij *et al.*, *Measurement of CP violation and the B_s^0 meson decay width difference with $B_s^0 \rightarrow J/\psi K^+ K^-$ and $B_s^0 \rightarrow J/\psi \pi^+ \pi^-$ decays*, Phys. Rev. **D87** (2013) 112010, [arXiv:1304.2600](https://arxiv.org/abs/1304.2600).

- [7] ATLAS Collaboration, G. Aad *et al.*, *Flavour tagged time dependent angular analysis of the $B_s \rightarrow J/\psi\phi$ decay and extraction of $\Delta\Gamma_s$ and the weak phase ϕ_s in ATLAS*, Phys. Rev. **D90** (2014) 052007, [arXiv:1407.1796](#).
- [8] CDF collaboration, T. Aaltonen *et al.*, *Measurement of the bottom-strange meson mixing phase in the full CDF data set*, Phys. Rev. Lett. **109** (2012) 171802, [arXiv:1208.2967](#).
- [9] D0 collaboration, V. M. Abazov *et al.*, *Measurement of the CP-violating phase $\phi_s^{J/\psi\phi}$ using the flavor-tagged decay $B_s^0 \rightarrow J/\psi\phi$ in 8 fb^{-1} of $p\bar{p}$ collisions*, Phys. Rev. **D85** (2012) 032006, [arXiv:1109.3166](#).
- [10] LHCb collaboration, R. Aaij *et al.*, *Measurement of the CP-violating phase ϕ_s in $\bar{B}_s^0 \rightarrow J/\psi\pi^+\pi^-$ decays*, Phys. Lett. **B736** (2014) 186, [arXiv:1405.4140](#).
- [11] S. Faller, R. Fleischer, and T. Mannel, *Precision physics with $B_s^0 \rightarrow J/\psi\phi$ at the LHC: the quest for new physics*, Phys. Rev. **D79** (2009) 014005, [arXiv:0810.4248](#).
- [12] LHCb collaboration, A. A. Alves Jr. *et al.*, *The LHCb detector at the LHC*, JINST **3** (2008) S08005.
- [13] R. Aaij *et al.*, *The LHCb trigger and its performance in 2011*, JINST **8** (2013) P04022, [arXiv:1211.3055](#).
- [14] S. Stone and L. Zhang, *S-waves and the measurement of CP violating phases in B_s^0 decays*, Phys. Rev. **D79** (2009) 074024, [arXiv:0812.2832](#).
- [15] D. Martinez Santos and F. Dupertuis, *Mass distributions marginalized over per-event errors*, Nucl. Instrum. Meth. **A764** (2014) 150, [arXiv:1312.5000](#).
- [16] LHCb collaboration, R. Aaij *et al.*, *Measurement of the flavour-specific CP-violating asymmetry a_{sl}^s in B_s^0 decays*, Phys. Lett. **B728** (2014) 607, [arXiv:1308.1048](#).
- [17] Y. Xie, *sFit: A method for background subtraction in maximum likelihood fit*, [arXiv:0905.0724](#).
- [18] LHCb collaboration, R. Aaij *et al.*, *Measurements of the B^+ , B^0 , B_s^0 meson and Λ_b^0 baryon lifetimes*, JHEP **04** (2014) 114, [arXiv:1402.2554](#).
- [19] LHCb collaboration, *Optimization and calibration of the same-side kaon tagging algorithm using hadronic B_s^0 decays in 2011 data*, LHCb-CONF-2012-033.
- [20] See supplementary material for details.
- [21] LHCb collaboration, R. Aaij *et al.*, *Precision measurement of the $B_s^0 - \bar{B}_s^0$ oscillation frequency in the decay $B_s^0 \rightarrow D_s^+\pi^-$* , New J. Phys. **15** (2013) 053021, [arXiv:1304.4741](#).

- [22] X. Liu, W. Wang, and Y. Xie, *Penguin pollution in $B \rightarrow J/\psi V$ decays and impact on the extraction of the $B_s - \bar{B}_s$ mixing phase*, Phys. Rev. **D89** (2014) 094010, [arXiv:1309.0313](#).
- [23] LHCb collaboration, R. Aaij *et al.*, *Observation of the decay $B_c^+ \rightarrow B_s^0 \pi^+$* , Phys. Rev. Lett. **111** (2013) 181801, [arXiv:1308.4544](#).
- [24] V. Kiselev, *Decays of the B_c meson*, [arXiv:hep-ph/0308214](#).

1 Supplementary material for PRL

Table 5: Statistical correlation matrix from the polarisation-independent fit.

	Γ_s	$\Delta\Gamma_s$	$ A_\perp ^2$	$ A_0 ^2$	δ_\parallel	δ_\perp	ϕ_s	$ \lambda $	Δm_s
Γ_s	+1.00	-0.45	+0.39	-0.31	-0.07	-0.02	+0.01	-0.01	+0.01
$\Delta\Gamma_s$		+1.00	-0.69	+0.65	+0.02	-0.03	-0.08	+0.02	-0.03
$ A_\perp ^2$			+1.00	-0.59	-0.29	-0.10	+0.04	-0.03	+0.00
$ A_0 ^2$				+1.00	-0.02	-0.04	-0.03	+0.02	-0.03
δ_\parallel					+1.00	+0.42	+0.01	+0.05	+0.05
δ_\perp						+1.00	+0.14	-0.17	+0.67
ϕ_s							+1.00	-0.02	+0.09
$ \lambda $								+1.00	-0.21
Δm_s									+1.00

Table 6: Total statistical and systematic correlation matrix from the polarisation-independent fit.

	Γ_s	$\Delta\Gamma_s$	$ A_\perp ^2$	$ A_0 ^2$	δ_\parallel	δ_\perp	ϕ_s	$ \lambda $	Δm_s
Γ_s	+1.00	-0.30	+0.25	-0.09	-0.08	-0.01	+0.01	-0.01	+0.03
$\Delta\Gamma_s$		+1.00	-0.59	+0.36	-0.06	-0.05	-0.08	+0.03	-0.00
$ A_\perp ^2$			+1.00	-0.70	+0.03	+0.08	+0.05	+0.00	+0.02
$ A_0 ^2$				+1.00	-0.38	-0.28	-0.04	-0.01	-0.05
δ_\parallel					+1.00	+0.47	+0.03	+0.00	+0.05
δ_\perp						+1.00	+0.15	-0.18	+0.64
ϕ_s							+1.00	-0.03	+0.09
$ \lambda $								+1.00	-0.21
Δm_s									+1.00

Table 7: Statistical correlation matrix for the ϕ_s^k and $|\lambda^k|$ parameters from the polarisation-dependent fit.

	$ \lambda^0 $	$ \lambda^\parallel/\lambda^0 $	$ \lambda^\perp/\lambda^0 $	$ \lambda^S/\lambda^0 $	ϕ_s^0	$\phi_s^\parallel - \phi_s^0$	$\phi_s^\perp - \phi_s^0$	$\phi_s^S - \phi_s^0$
$ \lambda^0 $	+1.00	-0.32	-0.59	-0.89	+0.01	-0.08	-0.06	+0.00
$ \lambda^\parallel/\lambda^0 $		+1.00	-0.23	+0.27	+0.00	+0.31	+0.16	+0.10
$ \lambda^\perp/\lambda^0 $			+1.00	+0.53	-0.02	+0.06	-0.29	-0.02
$ \lambda^S/\lambda^0 $				+1.00	-0.01	+0.07	+0.06	+0.22
ϕ_s^0					+1.00	-0.14	+0.13	+0.14
$\phi_s^\parallel - \phi_s^0$						+1.00	+0.52	+0.11
$\phi_s^\perp - \phi_s^0$							+1.00	+0.08
$\phi_s^S - \phi_s^0$								+1.00

Table 8: Total statistical and systematic correlation matrix for the ϕ_s^k and $|\lambda^k|$ parameters from the polarisation-dependent fit.

	$ \lambda^0 $	$ \lambda^\parallel/\lambda^0 $	$ \lambda^\perp/\lambda^0 $	$ \lambda^S/\lambda^0 $	ϕ_s^0	$\phi_s^\parallel - \phi_s^0$	$\phi_s^\perp - \phi_s^0$	$\phi_s^S - \phi_s^0$
$ \lambda^0 $	+1.00	-0.35	-0.56	-0.77	-0.00	-0.09	-0.07	-0.02
$ \lambda^\parallel/\lambda^0 $		+1.00	-0.23	+0.15	+0.02	+0.32	+0.17	+0.14
$ \lambda^\perp/\lambda^0 $			+1.00	+0.51	-0.02	+0.05	-0.29	-0.03
$ \lambda^S/\lambda^0 $				+1.00	-0.03	+0.03	+0.04	+0.18
ϕ_s^0					+1.00	-0.13	+0.13	+0.14
$\phi_s^\parallel - \phi_s^0$						+1.00	+0.51	+0.12
$\phi_s^\perp - \phi_s^0$							+1.00	+0.09
$\phi_s^S - \phi_s^0$								+1.00

Table 9: S-wave parameter estimates in each $m(K^+K^-)$ bin from the polarisation-independent fit. Only statistical uncertainties are shown.

Parameter	Value
F_{S1}	0.426 \pm 0.054
F_{S2}	0.059 \pm 0.017
F_{S3}	0.0101 \pm 0.0067
F_{S4}	0.0103 \pm 0.0061
F_{S5}	0.049 \pm 0.015
F_{S6}	0.193 \pm 0.025
$\delta_{S1} - \delta_\perp$	0.84 \pm 0.20
$\delta_{S2} - \delta_\perp$	2.15 \pm 0.28
$\delta_{S3} - \delta_\perp$	0.47 \pm 0.21
$\delta_{S4} - \delta_\perp$	-0.34 \pm 0.17
$\delta_{S5} - \delta_\perp$	-0.59 \pm 0.15
$\delta_{S6} - \delta_\perp$	-0.90 \pm 0.14

LHCb collaboration

R. Aaij⁴¹, B. Adeva³⁷, M. Adinolfi⁴⁶, A. Affolder⁵², Z. Ajaltouni⁵, S. Akar⁶, J. Albrecht⁹, F. Alessio³⁸, M. Alexander⁵¹, S. Ali⁴¹, G. Alkhazov³⁰, P. Alvarez Cartelle³⁷, A.A. Alves Jr^{25,38}, S. Amato², S. Amerio²², Y. Amhis⁷, L. An³, L. Anderlini^{17,g}, J. Anderson⁴⁰, R. Andreassen⁵⁷, M. Andreotti^{16,f}, J.E. Andrews⁵⁸, R.B. Appleby⁵⁴, O. Aquines Gutierrez¹⁰, F. Archilli³⁸, A. Artamonov³⁵, M. Artuso⁵⁹, E. Aslanides⁶, G. Auriemma^{25,n}, M. Baalouch⁵, S. Bachmann¹¹, J.J. Back⁴⁸, A. Badalov³⁶, C. Baesso⁶⁰, W. Baldini¹⁶, R.J. Barlow⁵⁴, C. Barschel³⁸, S. Barsuk⁷, W. Barter⁴⁷, V. Batozskaya²⁸, V. Battista³⁹, A. Bay³⁹, L. Beaucourt⁴, J. Beddow⁵¹, F. Bedeschi²³, I. Bediaga¹, S. Belogurov³¹, K. Belous³⁵, I. Belyaev³¹, E. Ben-Haim⁸, G. Bencivenni¹⁸, S. Benson³⁸, J. Benton⁴⁶, A. Berezhnoy³², R. Bernet⁴⁰, A. Bertolin²², M.-O. Bettler⁴⁷, M. van Beuzekom⁴¹, A. Bien¹¹, S. Bifani⁴⁵, T. Bird⁵⁴, A. Bizzeti^{17,i}, P.M. Bjørnstad⁵⁴, T. Blake⁴⁸, F. Blanc³⁹, J. Blouw¹⁰, S. Blusk⁵⁹, V. Bocci²⁵, A. Bondar³⁴, N. Bondar^{30,38}, W. Bonivento¹⁵, S. Borghi⁵⁴, A. Borgia⁵⁹, M. Borsato⁷, T.J.V. Bowcock⁵², E. Bowen⁴⁰, C. Bozzi¹⁶, D. Brett⁵⁴, M. Britsch¹⁰, T. Britton⁵⁹, J. Brodzicka⁵⁴, N.H. Brook⁴⁶, A. Bursche⁴⁰, J. Buytaert³⁸, S. Cadeddu¹⁵, R. Calabrese^{16,f}, M. Calvi^{20,k}, M. Calvo Gomez^{36,p}, P. Campana¹⁸, D. Campora Perez³⁸, A. Carbone^{14,d}, G. Carboni^{24,l}, R. Cardinale^{19,38,j}, A. Cardini¹⁵, L. Carson⁵⁰, K. Carvalho Akiba^{2,38}, RCM Casanova Mohr³⁶, G. Casse⁵², L. Cassina^{20,k}, L. Castillo Garcia³⁸, M. Cattaneo³⁸, Ch. Cauet⁹, R. Cenci^{23,t}, M. Charles⁸, Ph. Charpentier³⁸, M. Chefdeville⁴, S. Chen⁵⁴, S.-F. Cheung⁵⁵, N. Chiapolini⁴⁰, M. Chrzasczcz^{40,26}, X. Cid Vidal³⁸, G. Ciezarek⁴¹, P.E.L. Clarke⁵⁰, M. Clemencic³⁸, H.V. Cliff⁴⁷, J. Closier³⁸, V. Coco³⁸, J. Cogan⁶, E. Cogneras⁵, V. Cogoni¹⁵, L. Cojocariu²⁹, G. Collazuol²², P. Collins³⁸, A. Comerma-Montells¹¹, A. Contu^{15,38}, A. Cook⁴⁶, M. Coombes⁴⁶, S. Coquereau⁸, G. Corti³⁸, M. Corvo^{16,f}, I. Counts⁵⁶, B. Couturier³⁸, G.A. Cowan⁵⁰, D.C. Craik⁴⁸, A.C. Crocombe⁴⁸, M. Cruz Torres⁶⁰, S. Cunliffe⁵³, R. Currie⁵³, C. D'Ambrosio³⁸, J. Dalseno⁴⁶, P. David⁸, P.N.Y. David⁴¹, A. Davis⁵⁷, K. De Bruyn⁴¹, S. De Capua⁵⁴, M. De Cian¹¹, J.M. De Miranda¹, L. De Paula², W. De Silva⁵⁷, P. De Simone¹⁸, C.-T. Dean⁵¹, D. Decamp⁴, M. Deckenhoff⁹, L. Del Buono⁸, N. Déléage⁴, D. Derkach⁵⁵, O. Deschamps⁵, F. Dettori³⁸, A. Di Canto³⁸, A Di Domenico²⁵, H. Dijkstra³⁸, S. Donleavy⁵², F. Dordei¹¹, M. Dorigo³⁹, A. Dosil Suárez³⁷, D. Dossett⁴⁸, A. Dovbnya⁴³, K. Dreimanis⁵², G. Dujany⁵⁴, F. Dupertuis³⁹, P. Durante³⁸, R. Dzhelyadin³⁵, A. Dziurda²⁶, A. Dzyuba³⁰, S. Easo^{49,38}, U. Egede⁵³, V. Egorychev³¹, S. Eidelman³⁴, S. Eisenhardt⁵⁰, U. Eitschberger⁹, R. Ekelhof⁹, L. Eklund⁵¹, I. El Rifai⁵, Ch. Elsasser⁴⁰, S. Ely⁵⁹, S. Esen¹¹, H.-M. Evans⁴⁷, T. Evans⁵⁵, A. Falabella¹⁴, C. Färber¹¹, C. Farinelli⁴¹, N. Farley⁴⁵, S. Farry⁵², R. Fay⁵², D. Ferguson⁵⁰, V. Fernandez Albor³⁷, F. Ferreira Rodrigues¹, M. Ferro-Luzzi³⁸, S. Filippov³³, M. Fiore^{16,f}, M. Fiorini^{16,f}, M. Firlej²⁷, C. Fitzpatrick³⁹, T. Fiutowski²⁷, P. Fol⁵³, M. Fontana¹⁰, F. Fontanelli^{19,j}, R. Forty³⁸, O. Francisco², M. Frank³⁸, C. Frei³⁸, M. Frosini¹⁷, J. Fu^{21,38}, E. Furfaro^{24,l}, A. Gallas Torreira³⁷, D. Galli^{14,d}, S. Gallorini^{22,38}, S. Gambetta^{19,j}, M. Gandelman², P. Gandini⁵⁹, Y. Gao³, J. García Pardiñas³⁷, J. Garofoli⁵⁹, J. Garra Tico⁴⁷, L. Garrido³⁶, D. Gascon³⁶, C. Gaspar³⁸, U. Gastaldi¹⁶, R. Gauld⁵⁵, L. Gavardi⁹, G. Gazzoni⁵, A. Geraci^{21,v}, E. Gersabeck¹¹, M. Gersabeck⁵⁴, T. Gershon⁴⁸, Ph. Ghez⁴, A. Gianelle²², S. Gianì³⁹, V. Gibson⁴⁷, L. Giubega²⁹, V.V. Gligorov³⁸, C. Göbel⁶⁰, D. Golubkov³¹, A. Golutvin^{53,31,38}, A. Gomes^{1,a}, C. Gotti^{20,k}, M. Grabalosa Gándara⁵, R. Graciani Diaz³⁶, L.A. Granado Cardoso³⁸, E. Graugés³⁶, E. Graverini⁴⁰, G. Graziani¹⁷, A. Grecu²⁹, E. Greening⁵⁵, S. Gregson⁴⁷, P. Griffith⁴⁵, L. Grillo¹¹, O. Grünberg⁶³, B. Gui⁵⁹, E. Gushchin³³, Yu. Guz^{35,38}, T. Gys³⁸, C. Hadjivasiliou⁵⁹, G. Haefeli³⁹, C. Haen³⁸,

S.C. Haines⁴⁷, S. Hall⁵³, B. Hamilton⁵⁸, T. Hampson⁴⁶, X. Han¹¹, S. Hansmann-Menzemer¹¹,
 N. Harnew⁵⁵, S.T. Harnew⁴⁶, J. Harrison⁵⁴, J. He³⁸, T. Head³⁹, V. Heijne⁴¹, K. Hennessy⁵²,
 P. Henrard⁵, L. Henry⁸, J.A. Hernando Morata³⁷, E. van Herwijnen³⁸, M. Heß⁶³, A. Hicheur²,
 D. Hill⁵⁵, M. Hoballah⁵, C. Hombach⁵⁴, W. Hulsbergen⁴¹, N. Hussain⁵⁵, D. Hutchcroft⁵²,
 D. Hynds⁵¹, M. Idzik²⁷, P. Ilten⁵⁶, R. Jacobsson³⁸, A. Jaeger¹¹, J. Jalocha⁵⁵, E. Jans⁴¹,
 P. Jatou³⁹, A. Jawahery⁵⁸, F. Jing³, M. John⁵⁵, D. Johnson³⁸, C.R. Jones⁴⁷, C. Joram³⁸,
 B. Jost³⁸, N. Jurik⁵⁹, S. Kandybei⁴³, W. Kanso⁶, M. Karacson³⁸, T.M. Karbach³⁸,
 S. Karodia⁵¹, M. Kelsey⁵⁹, I.R. Kenyon⁴⁵, T. Ketel⁴², B. Khanji^{20,38,k}, C. Khurewathanakul³⁹,
 S. Klaver⁵⁴, K. Klimaszewski²⁸, O. Kochebina⁷, M. Kolpin¹¹, I. Komarov³⁹, R.F. Koopman⁴²,
 P. Koppenburg^{41,38}, M. Korolev³², L. Kravchuk³³, K. Kreplin¹¹, M. Kreps⁴⁸, G. Krocker¹¹,
 P. Krokovny³⁴, F. Kruse⁹, W. Kucewicz^{26,o}, M. Kucharczyk^{20,26,k}, V. Kudryavtsev³⁴,
 K. Kurek²⁸, T. Kvaratskheliya³¹, V.N. La Thi³⁹, D. Lacarrere³⁸, G. Lafferty⁵⁴, A. Lai¹⁵,
 D. Lambert⁵⁰, R.W. Lambert⁴², G. Lanfranchi¹⁸, C. Langenbruch⁴⁸, B. Langhans³⁸,
 T. Latham⁴⁸, C. Lazzeroni⁴⁵, R. Le Gac⁶, J. van Leerdam⁴¹, J.-P. Lees⁴, R. Lefèvre⁵,
 A. Leflat³², J. Lefrançois⁷, O. Leroy⁶, T. Lesiak²⁶, B. Leverington¹¹, Y. Li⁷,
 T. Likhomanenko⁶⁴, M. Liles⁵², R. Lindner³⁸, C. Linn³⁸, F. Lionetto⁴⁰, B. Liu¹⁵, S. Lohn³⁸,
 I. Longstaff⁵¹, J.H. Lopes², P. Lowdon⁴⁰, D. Lucchesi^{22,r}, H. Luo⁵⁰, A. Lupato²², E. Luppi^{16,f},
 O. Lupton⁵⁵, F. Machefert⁷, I.V. Machikhiliyan³¹, F. Maciuc²⁹, O. Maev³⁰, S. Malde⁵⁵,
 A. Malinin⁶⁴, G. Manca^{15,e}, G. Mancinelli⁶, A. Mapelli³⁸, J. Maratas⁵, J.F. Marchand⁴,
 U. Marconi¹⁴, C. Marin Benito³⁶, P. Marino^{23,t}, R. Märki³⁹, J. Marks¹¹, G. Martellotti²⁵,
 M. Martinelli³⁹, D. Martinez Santos⁴², F. Martinez Vidal⁶⁵, D. Martins Tostes²,
 A. Massafferri¹, R. Matev³⁸, Z. Mathe³⁸, C. Matteuzzi²⁰, A. Mazurov⁴⁵, M. McCann⁵³,
 J. McCarthy⁴⁵, A. McNab⁵⁴, R. McNulty¹², B. McSkelly⁵², B. Meadows⁵⁷, F. Meier⁹,
 M. Meissner¹¹, M. Merk⁴¹, D.A. Milanese⁶², M.-N. Minard⁴, N. Moggi¹⁴, J. Molina Rodriguez⁶⁰,
 S. Monteil⁵, M. Morandin²², P. Morawski²⁷, A. Mordà⁶, M.J. Morello^{23,t}, J. Moron²⁷,
 A.-B. Morris⁵⁰, R. Mountain⁵⁹, F. Muheim⁵⁰, K. Müller⁴⁰, M. Mussini¹⁴, B. Muster³⁹,
 P. Naik⁴⁶, T. Nakada³⁹, R. Nandakumar⁴⁹, I. Nasteva², M. Needham⁵⁰, N. Neri²¹,
 S. Neubert³⁸, N. Neufeld³⁸, M. Neuner¹¹, A.D. Nguyen³⁹, T.D. Nguyen³⁹, C. Nguyen-Mau^{39,q},
 M. Nicol⁷, V. Niess⁵, R. Niet⁹, N. Nikitin³², T. Nikodem¹¹, A. Novoselov³⁵, D.P. O’Hanlon⁴⁸,
 A. Oblakowska-Mucha²⁷, V. Obraztsov³⁵, S. Ogilvy⁵¹, O. Okhrimenko⁴⁴, R. Oldeman^{15,e},
 C.J.G. Onderwater⁶⁶, M. Orlandea²⁹, J.M. Otalora Goicochea², A. Otto³⁸, P. Owen⁵³,
 A. Oyanguren⁶⁵, B.K. Pal⁵⁹, A. Palano^{13,c}, F. Palombo^{21,u}, M. Palutan¹⁸, J. Panman³⁸,
 A. Papanestis^{49,38}, M. Pappagallo⁵¹, L.L. Pappalardo^{16,f}, C. Parkes⁵⁴, C.J. Parkinson^{9,45},
 G. Passaleva¹⁷, G.D. Patel⁵², M. Patel⁵³, C. Patrignani^{19,j}, A. Pearce⁵⁴, A. Pellegrino⁴¹,
 G. Penso^{25,m}, M. Pepe Altarelli³⁸, S. Perazzini^{14,d}, P. Perret⁵, L. Pescatore⁴⁵, E. Pesen⁶⁷,
 K. Petridis⁵³, A. Petrolini^{19,j}, E. Picatoste Olloqui³⁶, B. Pietrzyk⁴, T. Pilař⁴⁸, D. Pinci²⁵,
 A. Pistone¹⁹, S. Playfer⁵⁰, M. Plo Casasus³⁷, F. Polci⁸, A. Poluektov^{48,34}, I. Polyakov³¹,
 E. Polcarpo², A. Popov³⁵, D. Popov¹⁰, B. Popovici²⁹, C. Potterat², E. Price⁴⁶, J.D. Price⁵²,
 J. Prisciandaro³⁹, A. Pritchard⁵², C. Prouve⁴⁶, V. Pugatch⁴⁴, A. Puig Navarro³⁹, G. Punzi^{23,s},
 W. Qian⁴, B. Rachwal²⁶, J.H. Rademacker⁴⁶, B. Rakotomiaramanana³⁹, M. Rama²³,
 M.S. Rangel², I. Raniuk⁴³, N. Rauschmayr³⁸, G. Raven⁴², F. Redi⁵³, S. Reichert⁵⁴,
 M.M. Reid⁴⁸, A.C. dos Reis¹, S. Ricciardi⁴⁹, S. Richards⁴⁶, M. Rihl³⁸, K. Rinnert⁵²,
 V. Rives Molina³⁶, P. Robbe⁷, A.B. Rodrigues¹, E. Rodrigues⁵⁴, P. Rodriguez Perez⁵⁴,
 S. Roiser³⁸, V. Romanovsky³⁵, A. Romero Vidal³⁷, M. Rotondo²², J. Rouvinet³⁹, T. Rul³⁸,
 H. Ruiz³⁶, P. Ruiz Valls⁶⁵, J.J. Saborido Silva³⁷, N. Sagidova³⁰, P. Sail⁵¹, B. Saitta^{15,e},
 V. Salustino Guimaraes², C. Sanchez Mayordomo⁶⁵, B. Sanmartin Sedes³⁷, R. Santacesaria²⁵,

C. Santamarina Rios³⁷, E. Santovetti^{24,l}, A. Sarti^{18,m}, C. Satriano^{25,n}, A. Satta²⁴,
D.M. Saunders⁴⁶, D. Savrina^{31,32}, M. Schiller³⁸, H. Schindler³⁸, M. Schlupp⁹, M. Schmelling¹⁰,
B. Schmidt³⁸, O. Schneider³⁹, A. Schopper³⁸, M.-H. Schune⁷, R. Schwemmer³⁸, B. Sciascia¹⁸,
A. Sciubba^{25,m}, A. Semennikov³¹, I. Sepp⁵³, N. Serra⁴⁰, J. Serrano⁶, L. Sestini²², P. Seyfert¹¹,
M. Shapkin³⁵, I. Shapoval^{16,43,f}, Y. Shcheglov³⁰, T. Shears⁵², L. Shekhtman³⁴,
V. Shevchenko⁶⁴, A. Shires⁹, R. Silva Coutinho⁴⁸, G. Simi²², M. Sirendi⁴⁷, N. Skidmore⁴⁶,
I. Skillicorn⁵¹, T. Skwarnicki⁵⁹, N.A. Smith⁵², E. Smith^{55,49}, E. Smith⁵³, J. Smith⁴⁷,
M. Smith⁵⁴, H. Snoek⁴¹, M.D. Sokoloff⁵⁷, F.J.P. Soler⁵¹, F. Soomro³⁹, D. Souza⁴⁶,
B. Souza De Paula², B. Spaan⁹, P. Spradlin⁵¹, S. Sridharan³⁸, F. Stagni³⁸, M. Stahl¹¹,
S. Stahl¹¹, O. Steinkamp⁴⁰, O. Stenyakin³⁵, F. Sterpka⁵⁹, S. Stevenson⁵⁵, S. Stoica²⁹,
S. Stone⁵⁹, B. Storaci⁴⁰, S. Stracka^{23,t}, M. Straticiu²⁹, U. Straumann⁴⁰, R. Stroili²², L. Sun⁵⁷,
W. Sutcliffe⁵³, K. Swientek²⁷, S. Swientek⁹, V. Syropoulos⁴², M. Szczekowski²⁸,
P. Szczypka^{39,38}, T. Szumlak²⁷, S. T'Jampens⁴, M. Teklishyn⁷, G. Tellarini^{16,f}, F. Teubert³⁸,
C. Thomas⁵⁵, E. Thomas³⁸, J. van Tilburg⁴¹, V. Tisserand⁴, M. Tobin³⁹, J. Todd⁵⁷, S. Tolk⁴²,
L. Tomassetti^{16,f}, D. Tonelli³⁸, S. Topp-Joergensen⁵⁵, N. Torr⁵⁵, E. Tournefier⁴, S. Tourneur³⁹,
M.T. Tran³⁹, M. Tresch⁴⁰, A. Trisovic³⁸, A. Tsaregorodtsev⁶, P. Tsopelas⁴¹, N. Tuning⁴¹,
M. Ubeda Garcia³⁸, A. Ukleja²⁸, A. Ustyuzhanin⁶⁴, U. Uwer¹¹, C. Vacca¹⁵, V. Vagnoni¹⁴,
G. Valenti¹⁴, A. Vallier⁷, R. Vazquez Gomez¹⁸, P. Vazquez Regueiro³⁷, C. Vázquez Sierra³⁷,
S. Vecchi¹⁶, J.J. Velthuis⁴⁶, M. Veltri^{17,h}, G. Veneziano³⁹, M. Vesterinen¹¹,
JVVB Viana Barbosa³⁸, B. Viaud⁷, D. Vieira², M. Vieites Diaz³⁷, X. Vilasis-Cardona^{36,p},
A. Vollhardt⁴⁰, D. Volyanskyy¹⁰, D. Voong⁴⁶, A. Vorobyev³⁰, V. Vorobyev³⁴, C. Voß⁶³,
J.A. de Vries⁴¹, R. Waldi⁶³, C. Wallace⁴⁸, R. Wallace¹², J. Walsh²³, S. Wandernoth¹¹,
J. Wang⁵⁹, D.R. Ward⁴⁷, N.K. Watson⁴⁵, D. Websdale⁵³, M. Whitehead⁴⁸, D. Wiedner¹¹,
G. Wilkinson^{55,38}, M. Wilkinson⁵⁹, M.P. Williams⁴⁵, M. Williams⁵⁶, H.W. Wilschut⁶⁶,
F.F. Wilson⁴⁹, J. Wimberley⁵⁸, J. Wishahi⁹, W. Wislicki²⁸, M. Witek²⁶, G. Wormser⁷,
S.A. Wotton⁴⁷, S. Wright⁴⁷, K. Wyllie³⁸, Y. Xie⁶¹, Z. Xing⁵⁹, Z. Xu³⁹, Z. Yang³, X. Yuan³,
O. Yushchenko³⁵, M. Zangoli¹⁴, M. Zavertyaev^{10,b}, L. Zhang³, W.C. Zhang¹², Y. Zhang³,
A. Zhelezov¹¹, A. Zhokhov³¹, L. Zhong³.

¹Centro Brasileiro de Pesquisas Físicas (CBPF), Rio de Janeiro, Brazil

²Universidade Federal do Rio de Janeiro (UFRJ), Rio de Janeiro, Brazil

³Center for High Energy Physics, Tsinghua University, Beijing, China

⁴LAPP, Université de Savoie, CNRS/IN2P3, Annecy-Le-Vieux, France

⁵Clermont Université, Université Blaise Pascal, CNRS/IN2P3, LPC, Clermont-Ferrand, France

⁶CPPM, Aix-Marseille Université, CNRS/IN2P3, Marseille, France

⁷LAL, Université Paris-Sud, CNRS/IN2P3, Orsay, France

⁸LPNHE, Université Pierre et Marie Curie, Université Paris Diderot, CNRS/IN2P3, Paris, France

⁹Fakultät Physik, Technische Universität Dortmund, Dortmund, Germany

¹⁰Max-Planck-Institut für Kernphysik (MPIK), Heidelberg, Germany

¹¹Physikalisches Institut, Ruprecht-Karls-Universität Heidelberg, Heidelberg, Germany

¹²School of Physics, University College Dublin, Dublin, Ireland

¹³Sezione INFN di Bari, Bari, Italy

¹⁴Sezione INFN di Bologna, Bologna, Italy

¹⁵Sezione INFN di Cagliari, Cagliari, Italy

¹⁶Sezione INFN di Ferrara, Ferrara, Italy

¹⁷Sezione INFN di Firenze, Firenze, Italy

¹⁸Laboratori Nazionali dell'INFN di Frascati, Frascati, Italy

¹⁹Sezione INFN di Genova, Genova, Italy

- ²⁰ *Sezione INFN di Milano Bicocca, Milano, Italy*
- ²¹ *Sezione INFN di Milano, Milano, Italy*
- ²² *Sezione INFN di Padova, Padova, Italy*
- ²³ *Sezione INFN di Pisa, Pisa, Italy*
- ²⁴ *Sezione INFN di Roma Tor Vergata, Roma, Italy*
- ²⁵ *Sezione INFN di Roma La Sapienza, Roma, Italy*
- ²⁶ *Henryk Niewodniczanski Institute of Nuclear Physics Polish Academy of Sciences, Kraków, Poland*
- ²⁷ *AGH - University of Science and Technology, Faculty of Physics and Applied Computer Science, Kraków, Poland*
- ²⁸ *National Center for Nuclear Research (NCBJ), Warsaw, Poland*
- ²⁹ *Horia Hulubei National Institute of Physics and Nuclear Engineering, Bucharest-Magurele, Romania*
- ³⁰ *Petersburg Nuclear Physics Institute (PNPI), Gatchina, Russia*
- ³¹ *Institute of Theoretical and Experimental Physics (ITEP), Moscow, Russia*
- ³² *Institute of Nuclear Physics, Moscow State University (SINP MSU), Moscow, Russia*
- ³³ *Institute for Nuclear Research of the Russian Academy of Sciences (INR RAN), Moscow, Russia*
- ³⁴ *Budker Institute of Nuclear Physics (SB RAS) and Novosibirsk State University, Novosibirsk, Russia*
- ³⁵ *Institute for High Energy Physics (IHEP), Protvino, Russia*
- ³⁶ *Universitat de Barcelona, Barcelona, Spain*
- ³⁷ *Universidad de Santiago de Compostela, Santiago de Compostela, Spain*
- ³⁸ *European Organization for Nuclear Research (CERN), Geneva, Switzerland*
- ³⁹ *Ecole Polytechnique Fédérale de Lausanne (EPFL), Lausanne, Switzerland*
- ⁴⁰ *Physik-Institut, Universität Zürich, Zürich, Switzerland*
- ⁴¹ *Nikhef National Institute for Subatomic Physics, Amsterdam, The Netherlands*
- ⁴² *Nikhef National Institute for Subatomic Physics and VU University Amsterdam, Amsterdam, The Netherlands*
- ⁴³ *NSC Kharkiv Institute of Physics and Technology (NSC KIPT), Kharkiv, Ukraine*
- ⁴⁴ *Institute for Nuclear Research of the National Academy of Sciences (KINR), Kyiv, Ukraine*
- ⁴⁵ *University of Birmingham, Birmingham, United Kingdom*
- ⁴⁶ *H.H. Wills Physics Laboratory, University of Bristol, Bristol, United Kingdom*
- ⁴⁷ *Cavendish Laboratory, University of Cambridge, Cambridge, United Kingdom*
- ⁴⁸ *Department of Physics, University of Warwick, Coventry, United Kingdom*
- ⁴⁹ *STFC Rutherford Appleton Laboratory, Didcot, United Kingdom*
- ⁵⁰ *School of Physics and Astronomy, University of Edinburgh, Edinburgh, United Kingdom*
- ⁵¹ *School of Physics and Astronomy, University of Glasgow, Glasgow, United Kingdom*
- ⁵² *Oliver Lodge Laboratory, University of Liverpool, Liverpool, United Kingdom*
- ⁵³ *Imperial College London, London, United Kingdom*
- ⁵⁴ *School of Physics and Astronomy, University of Manchester, Manchester, United Kingdom*
- ⁵⁵ *Department of Physics, University of Oxford, Oxford, United Kingdom*
- ⁵⁶ *Massachusetts Institute of Technology, Cambridge, MA, United States*
- ⁵⁷ *University of Cincinnati, Cincinnati, OH, United States*
- ⁵⁸ *University of Maryland, College Park, MD, United States*
- ⁵⁹ *Syracuse University, Syracuse, NY, United States*
- ⁶⁰ *Pontifícia Universidade Católica do Rio de Janeiro (PUC-Rio), Rio de Janeiro, Brazil, associated to ²*
- ⁶¹ *Institute of Particle Physics, Central China Normal University, Wuhan, Hubei, China, associated to ³*
- ⁶² *Departamento de Física, Universidad Nacional de Colombia, Bogota, Colombia, associated to ⁸*
- ⁶³ *Institut für Physik, Universität Rostock, Rostock, Germany, associated to ¹¹*
- ⁶⁴ *National Research Centre Kurchatov Institute, Moscow, Russia, associated to ³¹*
- ⁶⁵ *Instituto de Física Corpuscular (IFIC), Universitat de Valencia-CSIC, Valencia, Spain, associated to ³⁶*
- ⁶⁶ *Van Swinderen Institute, University of Groningen, Groningen, The Netherlands, associated to ⁴¹*
- ⁶⁷ *Celal Bayar University, Manisa, Turkey, associated to ³⁸*

- ^a *Universidade Federal do Triângulo Mineiro (UFMT), Uberaba-MG, Brazil*
- ^b *P.N. Lebedev Physical Institute, Russian Academy of Science (LPI RAS), Moscow, Russia*
- ^c *Università di Bari, Bari, Italy*
- ^d *Università di Bologna, Bologna, Italy*
- ^e *Università di Cagliari, Cagliari, Italy*
- ^f *Università di Ferrara, Ferrara, Italy*
- ^g *Università di Firenze, Firenze, Italy*
- ^h *Università di Urbino, Urbino, Italy*
- ⁱ *Università di Modena e Reggio Emilia, Modena, Italy*
- ^j *Università di Genova, Genova, Italy*
- ^k *Università di Milano Bicocca, Milano, Italy*
- ^l *Università di Roma Tor Vergata, Roma, Italy*
- ^m *Università di Roma La Sapienza, Roma, Italy*
- ⁿ *Università della Basilicata, Potenza, Italy*
- ^o *AGH - University of Science and Technology, Faculty of Computer Science, Electronics and Telecommunications, Kraków, Poland*
- ^p *LIFAELS, La Salle, Universitat Ramon Llull, Barcelona, Spain*
- ^q *Hanoi University of Science, Hanoi, Viet Nam*
- ^r *Università di Padova, Padova, Italy*
- ^s *Università di Pisa, Pisa, Italy*
- ^t *Scuola Normale Superiore, Pisa, Italy*
- ^u *Università degli Studi di Milano, Milano, Italy*
- ^v *Politecnico di Milano, Milano, Italy*